Article:
North, S.M. and Armes, S.P. orcid.org/0000-0002-8289-6351 (2020) Aqueous solution behavior of stimulus-responsive poly(methacrylic acid)-poly(2-hydroxypropyl methacrylate) diblock copolymer nanoparticles. Polymer Chemistry, 11 (12). pp. 2147-2156. ISSN 1759-9954

https://doi.org/10.1039/d0py00061b

ARTICLE

Aqueous solution behavior of stimulus-responsive poly(methacrylic acid)-poly(2-hydroxypropyl methacrylate) diblock copolymer nanoparticles

Received 00th January 20xx,
Accepted 00th January 20xx

DOI: 10.1039/x0xx00000x

Shannon M. North and Steven P. Armes*

Abstract. Poly(methacrylic acid)-poly(2-hydroxypropyl methacrylate) ($PMAA_{50}$-$PHPMA_{237}$) diblock copolymer nanoparticles are synthesized via reversible addition-fragmentation chain transfer (RAFT) aqueous dispersion polymerization, which is an example of polymerization-induced self-assembly (PISA). These nanoparticles exhibit complex stimulus-responsive behavior in dilute aqueous solution. They undergo macroscopic precipitation at low pH owing to protonation of the PMAA steric stabilizer. However, adjusting the solution pH above the pK_a of 6.3 for the PMAA block ensures colloidal stability and confers thermoresponsive behavior. The degree of ionization of these anionic stabilizer chains increases at high pH, which leads to increasingly negative zeta potentials as judged by aqueous electrophoresis. Variable temperature dynamic light scattering (DLS) studies indicate the formation of progressively larger nanoparticles at higher temperatures, with TEM images providing evidence for weakly anisotropic nanoparticles at 50 °C. These observations are consistent with variable temperature ^{1}H NMR spectroscopy studies, which indicate gradual dehydration of the structure-directing PHPMA block. Rheology measurements on a 20% w/w copolymer dispersion indicate a critical gelation temperature of around 10 °C and a gel modulus (G') of approximately 1,000 Pa at 25 °C. Shear-induced polarized light imaging (SIPLI) studies confirm the presence of weakly anisotropic worm-like particles under such conditions.

Introduction

It is well-known that stimulus-responsive polymers are sensitive to changes in their external environment, such as pH,[1] temperature,[2] salt,[3] and light,[4] which in turn affects their chain conformation and/or solubility.[5–9] In principle, such stimulus-responsive polymers offer potential applications in stabilization, flocculation and inversion of colloidal dispersions, e.g. for catalysis,[10] water treatment,[11] water-borne coatings,[12,13] separation[14] and drug delivery.[15–18]

One of the most studied thermoresponsive synthetic polymers is poly(N-isopropylacrylamide) (PNIPAM).[19–30] This non-ionic water-soluble polymer undergoes a coil-to-globule transition in aqueous solution and becomes insoluble when heated above its lower critical solution temperature (LCST) of approximately 32°C. Incorporation of ionizable comonomers such as (meth)acrylic acid confers pH-responsive character.[30,31] This approach has been used to design a range of dual-responsive copolymer microgels that undergo reversible swelling on varying the solution pH and temperature.[32,33] 2-Hydroxypropyl methacrylate (HPMA) is water-miscible but the corresponding PHPMA homopolymer is water-insoluble. Thus, this commodity monomer offers a model system for understanding latex syntheses via aqueous dispersion polymerization.[34]

However, Madsen and co-workers demonstrated that, when conjugated to a sufficiently long hydrophilic block, PHPMA becomes water-dispersible and under such conditions it exhibits LCST-like thermoresponsive behavior. This enabled the design of new biocompatible hydrogels and micelles.[35–37]
There are many examples of pH-responsive polymers based on either weak polyacids such as poly(methacrylic acid) (PMAA)[38,39] and poly(acrylic acid)[40] or weak polybases such as poly(2-vinylpyridine) (P2VP)[41] or poly(2-(dimethylamino)ethyl methacrylate) (PDMA).[42,43] The former class is particularly relevant to the present study. Ionization of carboxylic acid groups confers polyelectrolytic character which causes PMAA to swell at high pH; this results in a conformational switch from compact (hyper-coiled) to highly extended chains.[44] Such anionic PMAA chains can act as an effective electrosteric stabilizer for colloidal particles.[4]

Polymerisation-induced self-assembly (PISA) is a highly versatile method for the synthesis of diblock copolymer nanoparticles in the form of concentrated dispersions.[46,47] In PISA, a second block is grown from a soluble precursor block in a solvent that is a poor solvent for the growing block. At some critical chain length, this drives in situ self-assembly to form nanoparticles, with the soluble block acting as the steric stabilizer and the insoluble block forming the nanoparticle cores. Once micellar nucleation occurs, there is a significant rate enhancement because the ensuing polymerization occurs within monomer-swollen micelles, which ensures a relatively high local monomer

Department of Chemistry, University of Sheffield, Dainton Building, Brook Hill, Sheffield, South Yorkshire S3 7HF, UK. (Correspondence to: s.p.armes@shef.ac.uk)
Electronic Supplementary Information (ESI) available: [details of any supplementary information available should be included here]. See DOI: 10.1039/x0xx00000x

concentration. Thus, relatively high monomer conversions can be achieved within short reaction times for such formulations. Moreover, this is a versatile and generic approach that enables the convenient and reproducible synthesis of diblock copolymer nano-objects in aqueous solution,[48–52] polar solvents (e.g. ethanol)[53,54] or non-polar media (e.g. *n*-alkanes).[55,56] The majority of PISA syntheses reported in the literature are based on reversible addition-fragmentation chain transfer (RAFT) polymerization.[47,57]

Both PAA and PMAA have been evaluated for aqueous PISA formulations. For example, Chaduc and co-workers reported various RAFT aqueous emulsion polymerization formulations using such electrosteric stabilizers.[58,59] Similarly, Cockram et al. used PMAA as a stabilizer block for the polymerization of various methacrylic monomers at pH 5.[60,61] PMAA and PAA have been also been used as steric stabilizer blocks for the synthesis of diblock copolymer nanoparticles via RAFT alcoholic dispersion polymerization.[62–64]

PHPMA has been used as a core-forming block for RAFT aqueous dispersion polymerization synthesis utilizing non-ionic steric stabilizers such as poly(glycerol monomethacrylate) or poly(ethylene glycol).[46,65–68] For such PISA syntheses, Blanazs et al. demonstrated that the PHPMA block can exhibit thermoresponsive character. Unusually, this block always remains hydrophobic but subtle changes in its degree of hydration on lowering the solution temperature are sufficient to induce a worm-to-sphere transition.[69] Thus this can be considered an 'LCST-like' transition.

However, such behavior is only observed within a limited molecular weight range.[46] Nevertheless, this thermal transition has led to the development of unique biocompatible hydrogels that can induce stasis in human stem cells.[70] More recently, it has also been exploited to design a single thermoresponsive diblock copolymer that can form either spheres, worms or vesicles in water simply by varying the solution temperature (rather than adjusting the diblock copolymer composition).[71]

In the present study, we examine a new PISA formulation based on the chain extension of a PMAA precursor via RAFT aqueous dispersion polymerization of HPMA (Scheme 1). In principle, the resulting $PMAA_{50}$-$PHPMA_{237}$ nanoparticles should exhibit both pH-responsive and thermoresponsive behavior in aqueous solution. This hypothesis is explored using a range of analytical techniques.

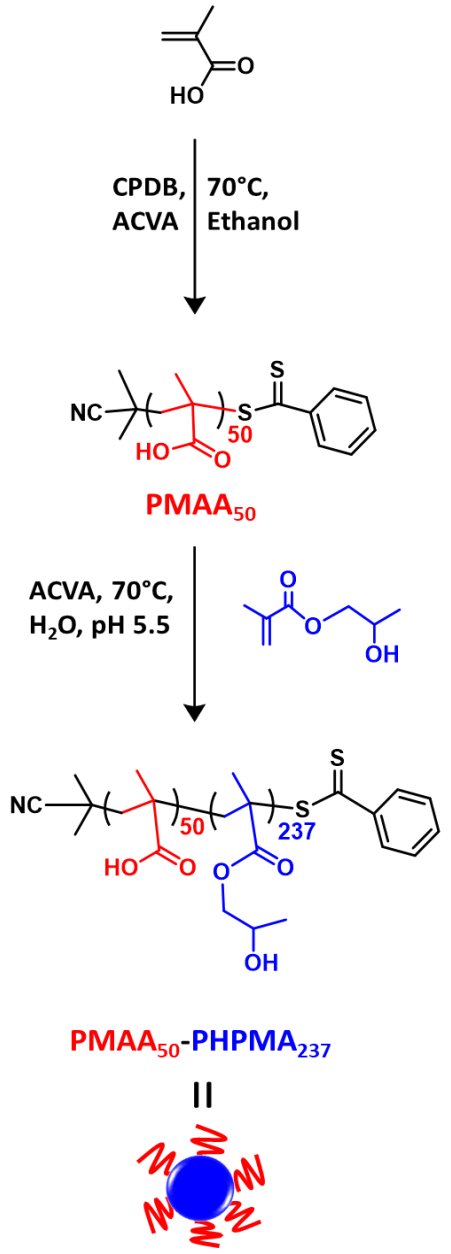

Scheme 1. RAFT solution polymerization of methacrylic acid (MAA) in ethanol using CPDB as a RAFT agent and 4,4'-azobis(4-cyanovaleric acid) (ACVA) as a free radical initiator to produce poly(methacrylic acid) (PMAA). This water-soluble precursor is then used for the RAFT aqueous dispersion polymerization of 2-hydroxypropyl methacrylate (HPMA) at 70 °C to produce spherical $PMAA_{50}$-$PHPMA_{237}$ diblock copolymer nanoparticles. The optimum solution pH for this PISA synthesis is pH 5.5.

Experimental

Materials

Methacrylic acid (MAA; 99%) and 4-cyanopropyl dithiobenzoate (CPDB) were purchased from Sigma-Aldrich (UK) and used without further purification. 4,4'-Azobis(4-cyanovaleric acid) (ACVA; 98%) was purchased from Alfa Aesar (UK) and used as received. HPMA was donated by GEO Specialty Chemicals. CD_3OD and dimethyl sulfoxide-d_6 was purchased from Goss Scientific Ltd (Cheshire, UK). Deuterium oxide (D_2O), sodium deuteroxide (NaOD) and deuterium chloride (DCl) were purchased from Sigma-Aldrich (Dorset, UK). All other solvents were purchased from Fisher Scientific (Loughborough, UK) and used as received. Deionized water was used for all experiments.

Synthesis of the poly(methacrylic acid) (PMAA) steric stabilizer

In a typical synthesis of the $PMAA_{50}$ precursor, a round-bottomed flask was charged with MAA (10.0 g, 116 mmol), 4-cyanopropyl dithiobenzoate (CPDB) (514 mg, 2.30 mmol), ACVA (130 mg, 0.46 mmol; CTA/initiator molar ratio = 5.0) and ethanol (16.0 g, 40% w/w). The sealed reaction vessel was purged with nitrogen gas and place in a pre-heated oil bath at 70 °C for 3 h. The resulting PMAA precursor (MAA conversion = 68%; M_n = 5 600 g mol^{-1}, M_w = 7 000 g

mol^{-1}, M_w/M_n = 1.26) was purified by precipitation into a ten-fold excess of diethyl ether (twice) and then isolated by lyophilization. A mean DP of 49 was estimated for this PMAA precursor using ^{1}H NMR spectroscopy by end-group analysis. Similarly, a mean DP of 50 was determined via UV spectroscopy using the 302 nm absorption band assigned to the dithiobenzoate RAFT chain-end for quantification with the aid of a Beer-Lambert calibration plot.

Synthesis of linear poly(methacrylic acid)-poly(2-hydroxypropyl methacrylate) diblock copolymer nanoparticles via RAFT aqueous dispersion polymerization

This RAFT aqueous dispersion polymerization synthesis was conducted at 20% w/w solids targeting $PMAA_{50}$-$PHPMA_{200}$. HPMA (0.60 g, 4.1 mmol), ACVA (1.45 mg, 5.2 µmol, CTA/initiator molar ratio = 4.0), and $PMAA_{50}$ macro-CTA (79.8 mg, 20.1 µmol) were dissolved in water (3.0 g). The solution pH was adjusted to 5.5 using an aqueous solution of 1 M NaOH. The pink reaction mixture was sealed in a round-bottomed flask, purged with nitrogen for 30 min, and then placed in a pre-heated oil bath at 70 °C for 2 h.

^{1}H NMR spectroscopy

All ^{1}H NMR spectra were recorded using a 400 MHz Bruker Avance-400 spectrometer using CD_3OD, D_2O, or dimethyl sulfoxide-d_6. Typically 64 scans were averaged per spectrum. NMR spectra were used to determine monomer conversions and also to estimate mean degrees of polymerization (DP) via end-group analysis.

UV spectroscopy

Absorption spectra were recorded using a Shimadzu UV-1800 spectrophotometer at 25 °C. A linear Beer-Lambert calibration plot was constructed using a series of solutions of CPDB (λ_{max} = 302 nm) dissolved in methanol at concentrations ranging between 1.59 and 14.8 g dm^{-3}. The $PMAA_{50}$ precursor was dissolved in methanol (0.122 g dm^{-3}) and its absorption maximum was recorded at 302 nm in order to calculate its mean degree of polymerization via end-group analysis. The same approach was used to determine the mean DP for the $PMAA_{50}$-$PHPMA_{237}$ nanoparticles, which were dried by lyophilization and then dissolved in methanol (26.4 mg copolymer in 10 ml) prior to analysis.

Variable temperature ^{1}H NMR studies of an aqueous dispersion of $PMAA_{50}$-$PHPMA_{237}$ nanoparticles

Nanoparticles were diluted to 1.0 % w/w in NaOD/D_2O (pD 10). The dispersion was cooled to 5 °C, equilibrated for 5 min and a spectrum was recorded. The temperature was then gradually increased to 50 °C and further spectra were recorded at 5 °C intervals, with 5 min being allowed for thermal equilibration in each case. A final spectrum was recorded after returning to 25 °C. A capillary tube containing 0.1 mol dm^{-3} pyridine dissolved in 1,1,2,2-tetrachloroethane-d_2 (lock solvent) was used as an external standard.

Exhaustive methylation protocol

$PMAA_{50}$ homopolymer was modified via exhaustive methylation of its carboxylic acid groups to form poly(methyl methacrylate). Excess trimethylsilyldiazomethane was added dropwise to a solution of $PMAA_{50}$ (20 mg) in THF (2.0 mL), until the yellow color persisted. This reaction solution was then stirred overnight until all THF had evaporated. The degree of methylation was determined to be 100% by ^{1}H NMR spectroscopy. This was determined by comparing the integrated backbone signal (0 – 2.5 ppm) to that of the new methoxy signal at 3.34 ppm.

Gel Permeation Chromatography (GPC)

The molecular weight distributions of the $PMAA_{50}$ precursor (after exhaustive methylation) and $PMAA_{50}$-$PHPMA_{237}$ diblock copolymer (without modification) were assessed using an Agilent Technologies PL GPC-50 system. The mobile phase was HPLC-grade THF containing 4.0% v/v glacial acetic acid at a flow rate of 1.0 ml min^{-1}. Molecular weights were calculated using a series of near-monodisperse poly(methyl methacrylate) calibration standards.

Dynamic Light Scattering (DLS)

0.10% w/w aqueous copolymer dispersions were analyzed in glass cuvettes at 25 °C using a Malvern Zetasizer NanoZS instrument. Scattered light was detected at 173° and the hydrodynamic diameters were calculated using the Stokes-Einstein equation. Data were averaged over three consecutive measurements comprising eleven runs per measurement.

Aqueous Electrophoresis

Measurements were performed using the same Malvern Zetasizer NanoZS instrument on a 0.10% w/w aqueous dispersion of nanoparticles in the presence of 1 mM KCl as background salt. The solution pH was adjusted using NaOH or HCl. The zeta potential was calculated from the electrophoretic mobility (µ) via the Henry equation using the Smoluchowsky approximation, which is valid for the electrophoretic determination of zeta potentials in aqueous media at moderate electrolyte concentrations.

Rheology Measurements

An AR-G2 rheometer equipped with a variable temperature Peltier plate and a 40 mm 2° aluminium cone was used for all experiments. An oscillatory mode was used to measure loss modulus (G"), and storage modulus (G') as a function of percentage strain amplitude, angular frequency, and temperature to assess critical gelation temperatures and gel strengths. Temperature sweeps were conducted using the same applied strain amplitude and at angular frequencies of 1 rad s^{-1}. Measurements were recorded at 1 °C intervals, allowing 5 min for thermal equilibration in each case.

Transmission electron microscopy (TEM)

Glow discharge-treated carbon-coated copper/palladium TEM grids (Agar Scientific, UK), tweezers, pipet tip, filter paper, 0.75% w/w aqueous uranyl formate solution, and a 1 mL stock solution of a 0.10 % w/w aqueous copolymer dispersion (adjusted to the desired pH using either 0.1 M NaOH or 0.1 M HCl), were equilibrated either in a fridge (set at either 5 °C or 10 °C), or at ambient temperature

(25 °C) or in a temperature-controlled oven (set at either 35 °C or 50 °C). A 0.2 µL droplet of the aqueous copolymer dispersion was deposited onto a TEM grid, and allowed to stand for 30 seconds at the desired temperature. Excess solution was then removed carefully using filter paper and each grid was allowed to dry at the same temperature. Finally, a 10 µL aliquot of the 0.75% w/w aqueous uranyl formate staining solution was placed onto the dried grid for 30 seconds at this temperature prior to careful drying using a vacuum hose.
TEM images were recorded using a Philips CM100 instrument operating at 100 kV and equipped with a Gatan 1k CCCD camera. ImageJ software was used to estimate mean nanoparticle diameters and standard deviations from TEM images (at least 100 nanoparticles were analyzed per sample).

Results and Discussion

Initially, a PMAA homopolymer precursor was prepared at 40% w/w via RAFT solution polymerization of MAA at 70 °C in ethanol using 2-cyanopropyl dithiobenzoate (CPDB) as a chain transfer agent (CTA). A DP of 50 was targeted and the polymerization was terminated after 3 h (65% conversion) to preserve RAFT chain-end functionality. After purification to remove excess monomer and other low molecular weight components, end-group analysis via ^{1}H NMR spectroscopy suggested a mean DP of 49. A calibration plot was produced using the CPDB RAFT agent dissolved in methanol. The molar extinction coefficient for the absorption maximum at 302 nm assigned to its dithiobenzoate end-group was determined to be 12600 ± 200 mol^{-1} dm^3 cm^{-1}.[72] Using this value, the mean DP of the PMAA homopolymer precursor was determined to be 50. The latter value is used throughout this manuscript, because UV spectroscopy is considered to be much more sensitive than ^{1}H NMR spectroscopy for such measurements. These data indicate a RAFT agent efficiency of around 67% for CPDB. This $PMAA_{50}$ precursor was then chain-extended via RAFT aqueous dispersion polymerization of HPMA, targeting a PHPMA block DP of 200 (Scheme 1). The diblock copolymer was analyzed by GPC using THF eluent containing 4% acetic acid, with the latter being added to the mobile phase to suppress ionization of the methacrylic acid groups.[61] The $PMAA_{50}$ macro-CTA required exhaustive methylation of its carboxylic acid groups to ensure THF solubility prior to GPC analysis. The M_n of this methylated precursor was determined to be 5 600 g mol^{-1}. Given that GPC calibration involved the use of a series of poly(methyl methacrylate) standards, this value is close to that expected (5 000 g mol^{-1}). Moreover, its M_w/M_n was determined to be 1.26, which indicates a reasonably well-controlled RAFT polymerization.
This $PMAA_{50}$ precursor was used to prepare $PMAA_{50}$-$PHPMA_{237}$ nanoparticles directly via RAFT aqueous dispersion polymerization of HPMA at 70 °C. Periodic sampling of the reaction mixture (with quenching achieved by dilution with concomitant cooling to 20 °C) enabled the kinetics of polymerization to be assessed by ^{1}H NMR spectroscopy. This was achieved by monitoring the disappearance of the vinyl proton signals at ~ 6 ppm relative to the methacrylic backbone signals at 0 – 2.5 ppm (Figure 1). This approach indicated that the HPMA polymerization was essentially complete within 2 h at 70 °C. The final DP for the PHPMA block can be calculated by

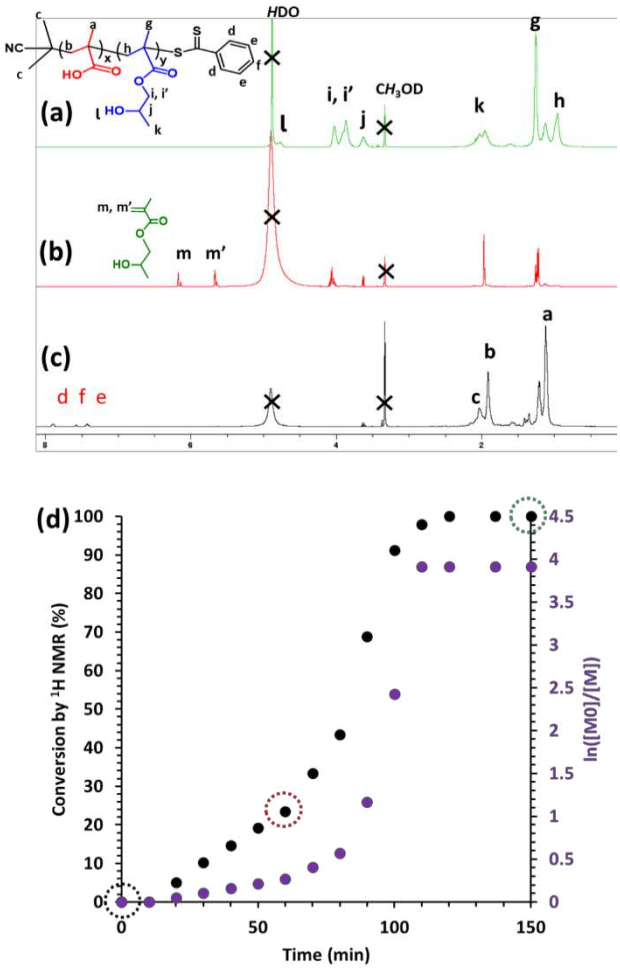

Figure 1. ^{1}H NMR spectra illustrating the gradual disappearance in the vinyl monomer signals at ~ 6 ppm and concomitant appearance of methacrylic backbone signals (0 – 2.5 ppm). (a) Full conversion of HPMA to afford $PMAA_{50}$-$PHPMA_{237}$ after 150 min, (b) 23% HPMA conversion after 60 min, (c) original PMAA precursor, (d) Conversion vs. time curve and corresponding semi-logarithmic plot indicating that the HPMA polymerization is complete within 2 h at 70 °C.

comparing the integrated oxymethylene PHPMA signal at ~ 4 ppm to that of the methacrylic backbone signals at 0 – 2.5 ppm. The complex PHPMA signals owe their existence to two HPMA isomers, which are present in a 75:25 ratio.[73]
The evolution in molecular weight over the course of the HPMA polymerization was followed by THF GPC (Figure 2). The molecular weight increased linearly with monomer conversion, as expected for a RAFT polymerisation. M_w/M_n values remain below 1.20 throughout the polymerization, and all chromatograms were unimodal, indicating a well-controlled RAFT polymerization. The final $PMAA_{50}$-$PHPMA_{237}$ diblock copolymer obtained at full monomer conversion had an apparent M_n of 36 000 g mol^{-1} and its M_w/M_n was 1.15.

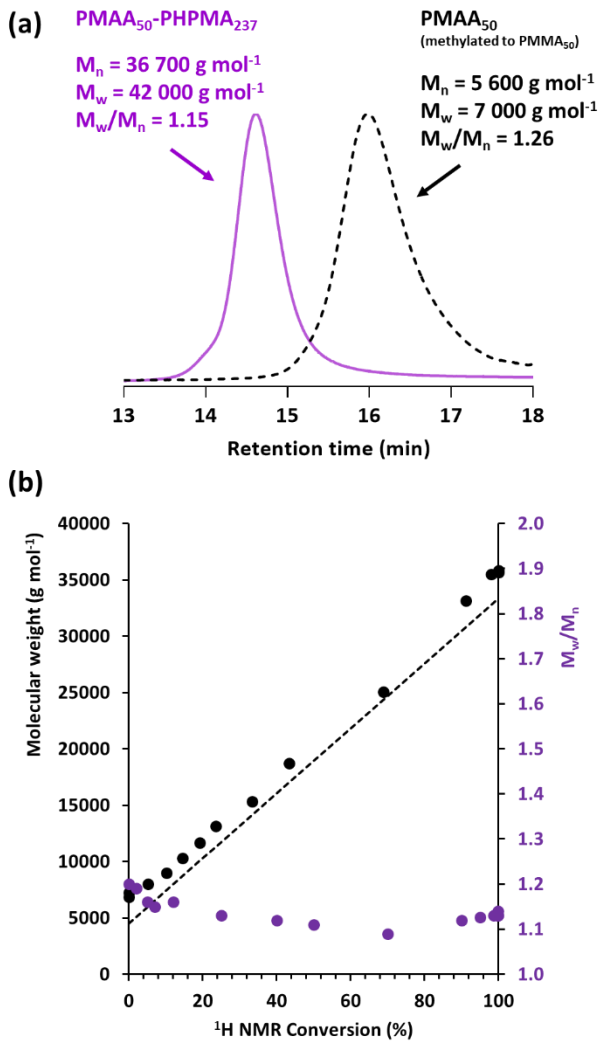

Figure 2. THF GPC curves recorded for a $PMAA_{50}$-$PHPMA_{237}$ diblock copolymer (and its corresponding $PMAA_{50}$ precursor, after exhaustive methylation to form $PMMA_{50}$) prepared at 20% w/w solids via RAFT aqueous dispersion polymerization of PHPMA at 70 °C. M_n values are expressed relative to a series of near-monodisperse poly(methyl methacrylate) calibration standards. Evolution of M_n and M_w/M_n with HPMA monomer conversion observed for this PISA synthesis.

The mean degree of polymerization for the PHPMA block was also determined using UV spectroscopy. This end-group analysis assumes that the λ_{max} and molar absorption coefficient (ε) remain unchanged during the course of the reaction (Figure 3).[74] The mean DP for the PHPMA block was calculated to be 237, whereas its target DP was 200. This suggests a RAFT agent efficiency of 84% for the RAFT aqueous dispersion polymerization step, which is comparable to that reported for other RAFT aqueous polymerizations.[75,76]

Aqueous electrophoresis measurements show that the nanoparticles become highly anionic above pH 6.3, exhibiting zeta potentials of approximately -45 mV owing to a high degree of ionization for the PMAA stabilizer chains (Figure 4). According to potentiometric acid titration studies (see Figure S1 in the Supporting Information), this pH corresponds to the pK_a for the $PMAA_{50}$-$PHPMA_{237}$ block of 6.27, which is slightly higher than the

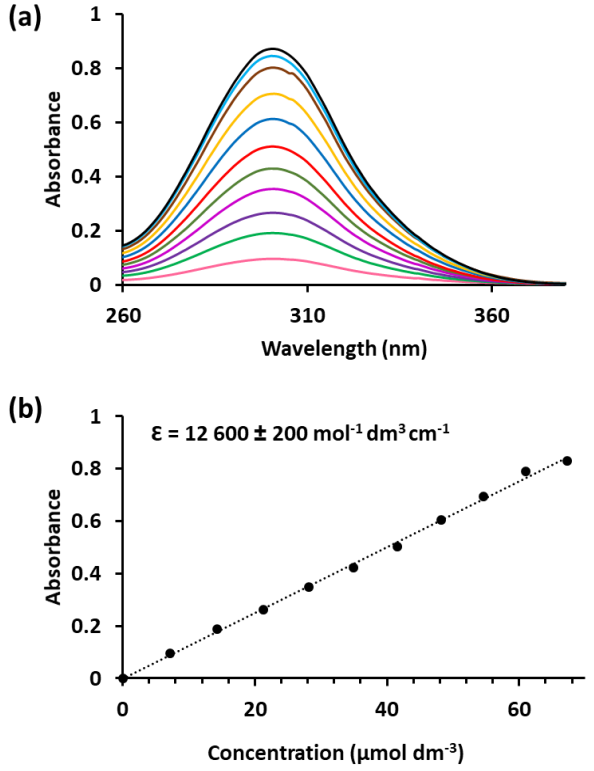

Figure 3. UV spectra recorded for CPDB dissolved in methanol for concentrations ranging from 7.2 µmol dm^{-3} (light pink spectrum) to 67.0 µmol dm^{-3} (black spectrum). (b) Determination of the molar absorption coefficient for CPDB using the Beer-Lambert law.

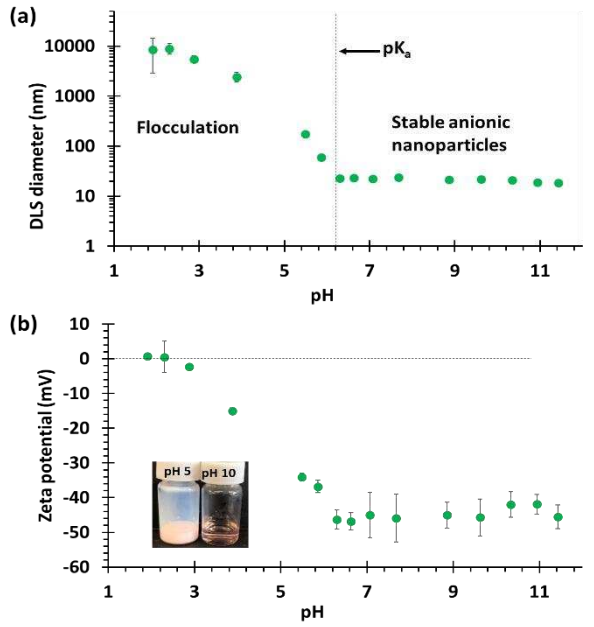

Figure 4. (a) Dynamic light scattering (DLS) studies of a 0.10 % aqueous dispersion of $PMAA_{50}$-$PHPMA_{237}$ nanoparticles at 25 °C. The large increase in hydrodynamic diameter observed below pH 6.3 is consistent with the onset of turbidity and observation of macroscopic precipitation below pH 6.3. (b) Zeta potential vs. pH curve obtained for a 0.10% aqueous dispersion of $PMAA_{50}$-$PHPMA_{237}$ nanoparticles. Inset digital photograph shows (left) the turbid dispersion obtained below the pK_a for the $PMAA_{50}$-$PHPMA_{237}$ diblock copolymer and (right) the relatively transparent dispersion formed above this pK_a. In both sets of experiments, the solution pH was adjusted using dilute aqueous solutions of either NaOH or HCl.

pK_a for the $PMAA_{50}$ precursor of 5.82; these experimental data lie close to the literature values reported for PMAA homopolymer and for diblock copolymer nanoparticles comprising PMAA coronas.[77,78] Below pH 6.3, the nanoparticles become progressively less anionic, exhibiting an isoelectric point (IEP) at approximately pH 2.3. Under such conditions, the neutral PMAA chains undergo a so-called 'hypercoiling' transition as a result of intramolecular hydrogen bonding interactions.[79]

DLS studies of a 0.10% w/w aqueous dispersion of these $PMAA_{50}$-$PHPMA_{237}$ nanoparticles indicate a significant increase in the scattered light intensity on lowering the solution pH (from ~1 000 kcps at pH 6.3 to ~ 20 000 kcps at pH 5.9). Visual inspection confirms that a substantial increase in turbidity occurs under such conditions, which is confirmed by turbidimetry studies (see Figure S2 in supporting information). As the solution pH is reduced further, the nanoparticles become colloidally unstable: the marked increase in apparent particle size observed at low pH indicates flocculation, because the nanoparticles no longer bear sufficient anionic surface charge to ensure their stabilization. On the other hand, relatively transparent nanoparticle dispersions are obtained above pH 6.3. The degree of ionization of the PMAA stabilizer chains exceeds 50% under such conditions, which is sufficient to ensure effective charge stabilization. According to the DLS data shown in Figure 4a, somewhat smaller nanoparticles are formed at higher pH. This size reduction is corroborated by TEM studies, which can only reveal the hydrophobic PHPMA cores (Figure 5). For example, the mean number-average diameter is 90 ± 33 nm at pH 5.5 but only 25 ± 5 nm at pH 10.5. This corresponds to a reduction in the mean aggregation number from 8140 to 174 (see Equations S1-S3 in Supporting Information for further details of these calculations). A comparison of the reduction in nanoparticle diameter with increasing pH observed by TEM and DLS is shown in Figure 5b. The latter technique oversizes relative to the former because it reports the intensity-average diameter, which always exceeds the number-average diameter for particle size distributions of finite width. This pH-dependent particle size is owed to the repulsion of PMAA chains when they become charged. Previously, this has been reported for the ionization of carboxylic end-groups, where the introduction of a single anionic charge was sufficient to change the packing parameter and induce a change in copolymer morphology.[80] In the present case, the introduction of multiple ionized acid groups on the PMAA stabilizer chains is expected to induce a significant reduction in the mean aggregation number and hence particle size. According to our previous studies, PHPMA only exhibits thermoresponsive character when conjugated to a suitably hydrophilic block.[35] For this reason, thermosensitive behavior is only observed for these sterically-stabilized nanoparticles when the PMAA stabilizer chains become highly ionized in alkaline solution. Thus, variable temperature ^{1}H NMR spectroscopy studies were conducted at pD 10 using $NaOD/D_2O$. These experiments confirm that the integrated signal for the two oxymethylene protons assigned to the core-forming PHPMA block at around 5 ppm become attenuated at elevated temperature (Figure 6). This

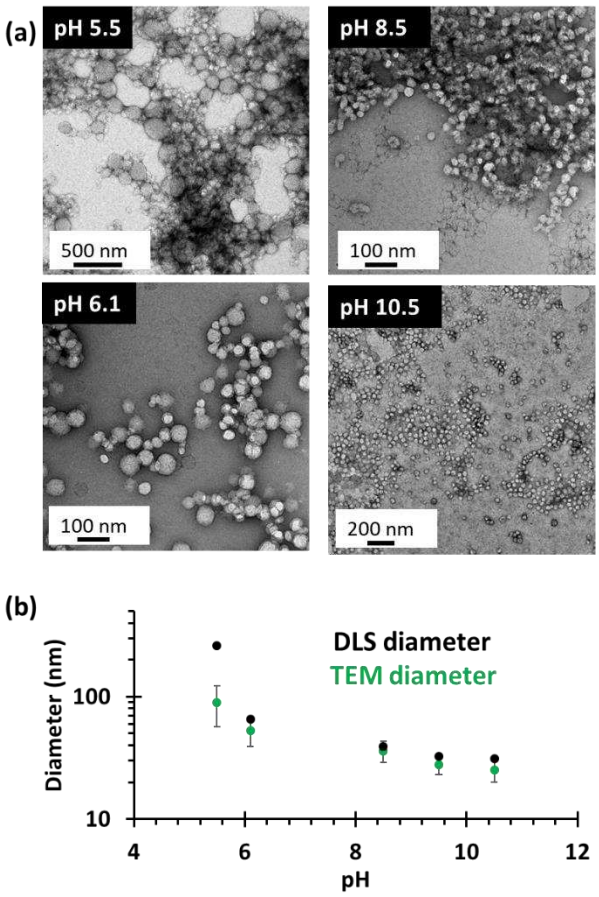

pH	TEM Diameter (nm)	TEM N_{agg}
5.5	90 ± 33	8140
6.1	53 ± 14	1662
8.5	36 ± 7	520
9.5	28 ± 5	245
10.5	25 ± 5	174

Figure 5. (a) Transmission electron microscopy images of $PMAA_{50}$-$PHPMA_{237}$ nanoparticles dried from 0.10 % aqueous solution between pH 5.5 and pH 10.5. (b) Variation of the mean particle diameter for these $PMAA_{50}$-$PHPMA_{237}$ nanoparticles as a function of pH as determined by TEM and DLS, respectively.

indicates that the weakly hydrophobic PHPMA block becomes progressively dehydrated on heating, as expected.[37] Since the intensity of the methacrylic backbone signals vary with temperature for both blocks, an external standard (pyridine dissolved in 1,1,2,2-tetrachloroethane-d_2) was used to monitor the extent of dehydration of this oxymethylene signal. The degree of hydration of the PHPMA chains is estimated to be approximately 75% at 5 °C.[37] However, gradual dehydration to around 37% is observed on heating to 25 °C, with this value remaining more or less constant up to 50 °C. These observations are consistent with prior reports for diblock copolymer nanoparticles comprising thermoresponsive PHPMA core-forming chains.[69,71,81]

These variable temperature NMR experiments are consistent with DLS studies (Figure 7). A very low count rate (or scattered light intensity) is observed for this aqueous copolymer dispersion at 2 °C

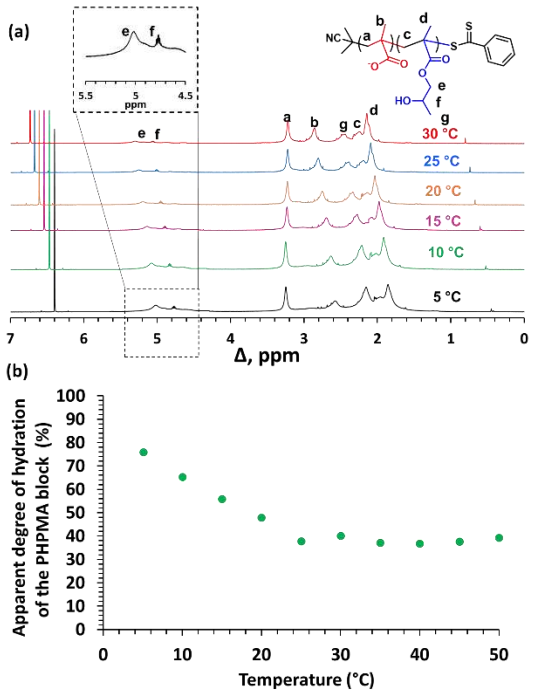

Figure 6. (a) ^{1}H NMR spectra recorded for $PMAA_{50}$-$PHPMA_{237}$ nanoparticles dispersed in NaOD/D_2O (pD 10) between 5 °C and 30 °C using an external standard to monitor the systematic reduction in PHPMA signal intensity that occurs on heating (see signals e and f at 5.0 and 4.57 ppm). (b) Relative degree of hydration for the PHPMA block calculated from 5 °C to 50 °C.

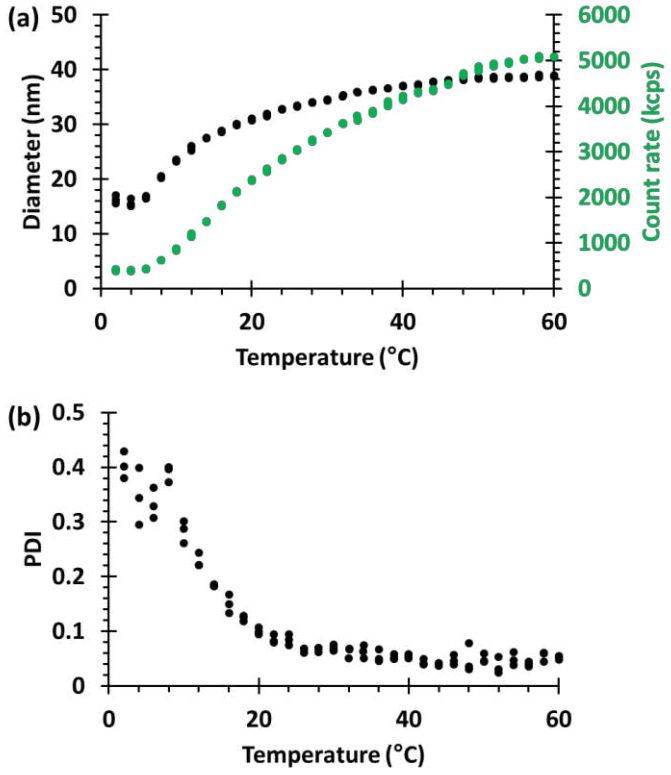

Figure 7. Variation in (a) intensity-average diameter and count rate and (b) polydispersity index (PDI) with temperature as determined by DLS studies of a 0.10% w/w aqueous dispersion of $PMAA_{50}$-$PHPMA_{237}$ nanoparticles at pH 10.

and the apparent mean diameter is only 15 nm under such conditions. As the solution temperature is increased, the core-forming PHPMA block becomes progressively more hydrophobic. This leads to a gradual increase in the size of the nanoparticles, which suggests that the copolymer chains are close to being molecularly dissolved under such conditions. As the solution temperature is increased, the core-forming PHPMA block becomes progressively more hydrophobic. This leads to a gradual increase in nanoparticle size, with an intensity-average diameter of 41 nm being observed at 50 °C.

TEM studies confirm this increase in particle size (Figure 8). The copolymer chains are close to molecular dissolution at 5 °C, so no nanoparticles are observed at this temperature.[37] The nanoparticle core diameter is 20 ± 3 nm at 10 °C and 35 ± 5 nm at 50 °C. This indicates a significant increase in mean aggregation number from 89 to 1840. These number-average diameters are consistent with the (larger) intensity-average diameters reported by DLS. The TEM

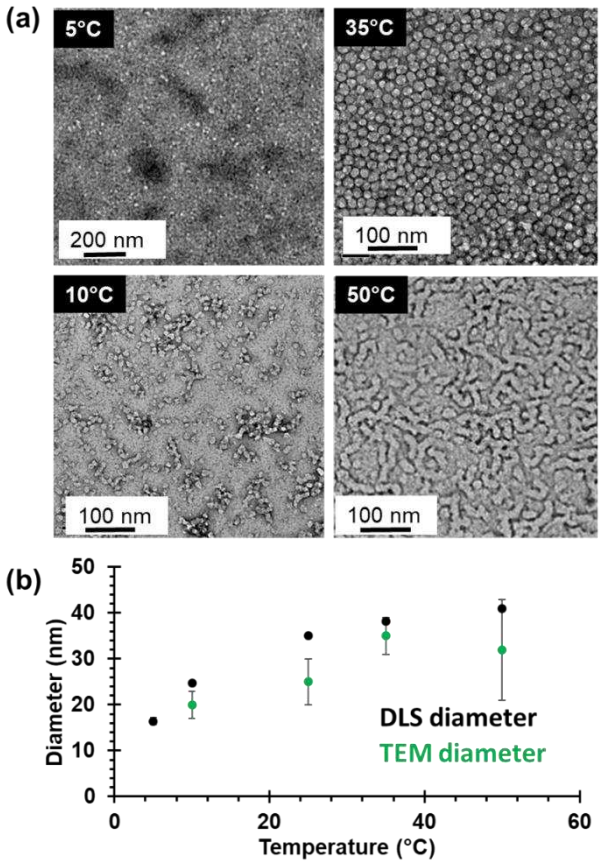

Temperature (°C)	TEM Diameter (nm)	TEM N_{agg}
5	-	
10	20 ± 3	89
25	25 ± 5	174
35	35 ± 5	479
50	Width = 35 ± 11 Length = 95 ± 11	1840

Figure 8. (a) Transmission electron microscopy images recorded after drying 0.10% aqueous dispersions of $PMAA_{50}$-$PHPMA_{237}$ nanoparticles at pH 10 at temperatures ranging from 2 °C to 50 °C. (b) Effect of varying the solution temperature on mean particle diameter as determined by TEM (green data set) and DLS (black data set) studies.

image obtained when drying this aqueous copolymer dispersion at 50 °C indicates the formation of short worms. This thermally-induced sphere-to-worm transition is supported by shear-induced polar light imaging (SIPLI) experiments: birefringence is observed at 50 °C which indicates alignment of these weakly anisotropic nanoparticles (see Figure S3 in the Supporting Information).[60,82] Finally, temperature-dependent rheology measurements were performed as a function of temperature on the 20 % w/w aqueous copolymer dispersion, which forms a free-standing gel (G' ~ 1 000 Pa) above 25 °C at pH 10. The critical gelation temperature (CGT) is estimated to be 10 °C for this copolymer dispersion (see Figure S4). The complex pH and thermoresponsive behavior exhibited by $PMAA_{50}$-$PHPMA_{237}$ nanoparticles in aqueous solution is summarized in Scheme 2.

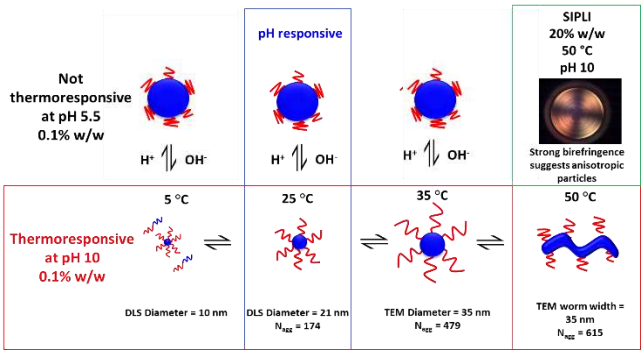

Scheme 2. Schematic representation of the stimulus-responsive behavior of $PMAA_{50}$-$PHPMA_{237}$ nanoparticles in aqueous solution. Relatively large, polydisperse spheres are formed at pH 5.5, which is the solution pH used for the RAFT aqueous dispersion polymerization of HPMA. At pH 10, the $PMAA_{50}$ stabilizer block becomes much more anionic, which leads to the formation of relatively small spherical nanoparticles at 5 °C. On increasing the solution temperature, these spheres grow in size and weakly anisotropic worms are formed at 50 °C, confirmed by SIPLI measurements (see Figure S3 in the Supporting Information).

Conclusions

A new amphiphilic $PMAA_{50}$-$PHPMA_{237}$ diblock copolymer has been prepared by RAFT aqueous dispersion polymerization of HPMA at pH 5.5. In dilute aqueous solution, the as-synthesized sterically-stabilized particles are relatively large and polydisperse because the mean degree of ionization of the PMAA block (pK_a ~ 6.3) is relatively low under such conditions. Lowering the solution pH leads to macroscopic precipitation owing to loss of their anionic surface charge. However, in alkaline solution the PMAA chains become highly anionic, which leads to the formation of relatively small thermoresponsive nanoparticles. Thus, molecularly-dissolved diblock copolymer chains are formed at 5 °C, rather than nanoparticles. At higher temperatures (10 - 35 °C), DLS, TEM and NMR studies indicate that the weakly hydrophobic PHPMA chains become progressively more dehydrated, which drives the formation of relatively small nanoparticles of gradually increasing aggregation number and size. At 50 °C, TEM studies indicate the formation of weakly anisotropic worm-like nanoparticles. At higher copolymer concentration (20% w/w), rheological studies indicate the formation of a free-standing transparent gel above 10 °C when the solution pH exceeds 6.3.

Supporting Information Available

Potentiometric acid titration data for $PMAA_{50}$ homopolymer and $PMAA_{50}$-$PHPMA_{237}$ diblock copolymer, turbidimetry studies at varying pH, calculation of the mean aggregation number, and temperature-dependent oscillatory rheology data and SIPLI studies.

Conflicts of interest

There are no conflicts to declare.

Acknowledgements

EPSRC is thanked for funding a CDT PhD studentship. Lubrizol is thanked for financial support of this PhD project. Dr. Sandra Van Meurs is acknowledged for her help in acquiring the variable temperature ^{1}H NMR data. Prof. Armes acknowledges a four-year EPSRC Established Career Particle Technology Fellowship (EP/R003009).

Notes and references

1 G. Kocak, C. Tuncer and V. Bütün, *Polym. Chem.* 2017, **8**, 144–176.
2 D. Roy, W. L. A. Brooks and B. S. Sumerlin, *Chem. Soc. Rev.* 2013, **42**, 7214–7243.
3 V. Kozlovskaya, E. Kharlampieva, M. L. Mansfield and S. A. Sukhishvili, *Chem. Mater*. 2006, **18**, 328–336.
4 O. Bertrand and J. F. Gohy, *Polym. Chem*. 2017, **8**, 52–73.
5 H. G. Schild, *Prog. Polym. Sci.* 1992, **17**, 163-249.
6 M. A. Cohen Stuart, W. T. S. Huck, J. Genzer, M. Müller, C. Ober, M. Stamm, G. B. Sukhorukov, I. Szleifer, V. V. Tsukruk, M. Urban, F. Winnik, S. Zauscher, I. Luzinov and S. Minko, *Nat. Mater.* 2010, **9**, 101–113.
7 J. F. Gohy and Y. Zhao, *Chem. Soc. Rev*. 2013, **42**, 7117–7129.
8 M. Arotçaréna, B. Heise, S. Ishaya and A. Laschewsky, *J. Am. Chem. Soc.* 2002, **124**, 3787–3793.
9 J. Du, Y. Tang, A. L. Lewis and S. P. Armes, *J. Am. Chem. Soc*. 2005, **127**, 17982–17983.
10 T. Chen, Z. Xu, L. Zhou, L. Hua, S. Zhang, J. Wang, *Tetrahedron Lett.* 2019, **60**, 419–422.
11 R. Wei, W. Song, F. Yang, J. Zhou, M. Zhang, X. Zhang, W. Zhao, C. Zhao, *Ind. Eng. Chem. Res*. 2018, **57**, 8209–8219.
12 C. Tso, C. Zhung, Y. Shih, Y.- M. Tseng, S. Wu, R. Doong, *Water Sci. Technol.* 2010, **61**, 127-133.
13 J. Cesarano, I. A. Aksay, A. Bleier, *J. Am. Ceram. Soc*. 1988, **71**, 250–255.
14 J. Ng, I. Osborn, D. Harbottle, Q. Liu, J. H. Masliyah, Z. Xu, *Environ. Sci. Technol.* 2019, **53**, 6436-6443
15 S. Mura, J. Nicolas, P. Couvreur, *Nat. Mater.* 2013, **12**, 991–1003.
16 S. Guragain, B. P. Bastakoti, V. Malgras, K. Nakashima, Y. Yamauchi, *Chem. Eur. J.* 2015, **21**, 13164–13174.
17 A. S. Hoffman, *Adv. Drug Deliv. Rev.* 2013, 65, 10–16.

18 Y. Bae, S. Fukushima, A. Harada, K. Kataoka, *Angew. Chem. Int. Ed.* 2003, **42**, 4640–4643.
19 A. Halperin, M. Kröger, F. M. Winnik, *Angew. Chem. Int. Ed.* 2015, **54**, 15342–15367.
20 R. Pelton, *Adv. Colloid Interface Sci.* 2000, **85**, 1–33.
21 Y. Zhang, S. Furyk, D. E. Bergbreiter, P. S. Cremer, *J. Am. Chem. Soc.* 2005, **127**, 14505–14510.
22 M. Heskins, J. E. Guillet, *J. Macromol. Sci. Part A - Chem.* 1968, **2**, 1441–1455.
23 C. de las Heras Alarcón, S. Pennadam, C. Alexander, *Chem. Soc. Rev.* 2005, **34**, 276-285.
24 H. Senff, W. Richtering, *J. Chem. Phys.* 1999, **111**, 1705–1711.
25 R. Liu, M. Fraylich, B. R. Saunders, *Colloid Polym. Sci.* 2009, **287**, 627–643.
26 M. Stieger, W. Richtering, J. S. Pedersen, P. Lindner, *J. Chem. Phys.* 2004, **120**, 6197–6206.
27 A. A. Steinschulte, A. Scotti, K. Rahimi, O. Nevskyi, A. Oppermann, S. Schneider, S. Bochenek, M. F. Schulte, K. Geisel, F. Jansen, A. Jung, S. Mallmann, R. Winter, W. Richtering, S. Woll, R. Schweins, N. J. Warren, F. A. Plamper, *Adv. Mater.* 2017, **29**, 1703495
28 C. A. Figg, A. Simula, K. A. Gebre, B. S. Tucker, D. M. Haddleton and B. S. Sumerlin, *Chem. Sci*. 2015, **6**, 1230–1236.
29 V. A. Bobrin, M. J. Monteiro, *J. Am. Chem. Soc.* 2015, **137**, 15652–15655.
30 D. E. Bergbreiter, B. L. Case, Y.-S. Liu, J. W. Caraway, *Macromolecules* 1998, **31**, 6053–6062.
31 T. Hoare and R. Pelton, *Macromolecules* 2004, **37**, 2544–2550.
32 B. R. Saunders, H. M. Crowther, B. Vincent, *Macromolecules* 2002, **30**, 482–487.
33 B. R. Saunders, *Langmuir* 2004, **20**, 3925–3932.
34 A. M. I. Ali, P. Pareek, L. Sewell, A. Schmid, S. Fujii, S. P. Armes, I. M. Shirley, *Soft Matter* 2007, **3**, 1003–1013.
35 J. Madsen, S. P. Armes, A. L. Lewis, *Macromolecules* 2006, *39*, 7455–7457.
36 J. Madsen, S. P. Armes, K. Bertal, S. Macneil, A. L. Lewis, *Biomacromolecules* 2009, **10**, 1875–1887.
37 J. Madsen, S. P. Armes, K. Bertal, H. Lomas, S. Macneil, A. L. Lewis, *Biomacromolecules* 2008, **9**, 2265–2275.
38 X. Liu, D. Yu, C. Jin, X. Song, J. Cheng, X. Zhao, X. Qi, G. Zhang, *New J. Chem.* 2014, **38**, 4830–4836.
39 C. Fernyhough, A. J. Ryan, G. Battaglia, *Soft Matter* 2009, **5**, 1674–1682.
40 S. L. Canning, J. M. F. Ferner, N. M. Mangham, T. J. Wear, S. W. Reynolds, J. Morgan, J. P. A. Fairclough, S. M. King, T. Swift, M. Geoghegan and S. Rimmer, *Polym. Chem*. 2018, **9**, 5617–5629.
41 J. Yin, D. Dupin, J. Li, S. P. Armes, S. Liu, *Langmuir* 2008, **24**, 9334–9340.
42 K. Sakai, E. G. Smith, G. B. Webber, M. Baker, E. J. Wanless, V. Bütün, S. P. Armes, S. Biggs, *J. Colloid Interface Sci.* 2007, **314**, 381–388.
43 P. G. Falireas, M. Vamvakaki, *Macromolecules* 2018, **51**, 6848–6858.
44 L. Ruiz-Pérez, A. Pryke, M. Sommer, G. Battaglia, I. Soutar, L. Swanson and M. Geoghan, *Macromolecules* 2008, **41**, 2203–2211.
45 Z. Qu, H. Xu, H. Gu, *ACS Appl. Mater. Interfaces* 2015, **7**, 14537–14551.
46 N. J. Warren, M. J. Derry, O. O. Mykhaylyk, J. R. Lovett, L. P. D. Ratcliffe, V. Ladmiral, A. Blanazs, L. A. Fielding, S. P. Armes, *Macromolecules* 2018, **51**, 8357–8371.
47 V. J. Cunningham, L. P. D. Ratcliffe, A. Blanazs, N. J. Warren, A. J. Smith, O. O. Mykhaylyk, S. P. Armes, *Polym. Chem*. 2014, **5**, 6307–6317.
48 N. J. Warren, S. P. Armes, *J. Am. Chem. Soc.* 2014, **136**, 10174–10185.
49 A. Blanazs, A. J. Ryan, S. P. Armes, *Macromolecules* 2012, **45**, 5099–5107.
50 J. Rieger, C. Grazon, B. Charleux, D. Alaimo, C. J. Jerome, J. Polym. Sci.Part A 2009, 47, 2373 – 2390
51 Z. An, Q. Shi, W. Tang, C. K. Tsung, C. J. Hawker, G. D. Stucky, *J. Am. Chem. Soc*. 2007, **129**, 14493 – 14499.
52 G. Delaittre, M. Save, B. Charleux, *Macromol. Rapid Commun*. 2007, **28**, 1528 – 1533.
53 M. Semsarilar, V. Ladmiral, A. Blanazs, S. P. Armes, *Langmuir* 2012, **28**, 914–922.
54 E. R. Jones, M. Semsarilar, A. Blanazs, S. P. Armes, *Macromolecules* 2012, **45**, 5091–5098.
55 M. J. Derry, L. A. Fielding, S. P. Armes, *Prog. Polym. Sci.* 2016, **52**, 1–18.
56 G. N. Smith, L. L. E. Mears, Rogers, S. E. Rogers and S. P. Armes, *Chem. Sci.* 2018, **9**, 922–934.
57 B. Charleux, G. Delaittre, J. Rieger, F. D'Agosto, *Macromolecules* 2012, **45**, 6753–6765.
58 I. Chaduc, M. Girod, R. Antoine, B. Charleux, F. D'Agosto, M. Lansalot, *Macromolecules* 2012, **45**, 5881–5893.
59 I. Chaduc, A. Crepet, O. Boyron, B. Charleux, F. D'Agosto, M. Lansalot, *Macromolecules* 2013, **46**, 6013–6023.
60 A. A. Cockram, T. J. Neal, M. J. Derry, O. O. Mykhaylyk, N. S. J. Williams, M. W. Murray, S. N. Emmett, S. P. Armes, *Macromolecules* 2017, **50**, 796–802.
61 A. A. Cockram, R. D. Bradley, S. A. Lynch, P. C. D. Fleming, N. S. J. Williams, S. N. Emmett and S. P. Armes, *React. Chem. Eng*. 2018, **3**, 645–657.
62 L. Upadhyaya, M. Semsarilar, S. Nehache, D. Cot, R. Fernández-Pacheco, G. Martinez, R. Mallada, A. Deratani, D. Quemener, *Macromolecules* 2016, **49,** 7908–7916.
63 M. Semsarilar, V. Ladmiral, A. Blanazs, S. P. Armes *Polym. Chem.* 2014*,* **5** 3466–3475.
64 S. L. Canning, V. J. Cunningham, L. P. D. Ratcliffe and S. P. Armes, *Polym. Chem.* 2017, **8**, 4811–4821.
65 L. D. Blackman, K. E. B. Doncom, M. I. Gibson and R. K. O'Reilly, *Polym. Chem*. 2017, **8**, 2860–2871.
66 M. Williams, N. J. W. Penfold, J. R. Lovett, N. J. Warren, C. W. I. Douglas, N. Doroshenko, P. Verstraete, J.Smets, S. P. Armes, *Polym. Chem*. 2016, **7**, 3864–3873.
67 J. Tan, Q. Xu, Y. Zhang, C. Huang, X. Li, J. He, L. Zhang, *Macromolecules* 2018, **51**, 7396–7406.
68 K. Ren, J. Perez-Mercader, *Polym. Chem*. 2017, **8**, 3548–3552.
69 A. Blanazs, R. Verber, O. O. Mykhaylyk, A. J. Ryan, J. Z. Heath, C. W. I. Douglas, S. P. Armes, *J. Am. Chem. Soc*. 2012, **134**, 9741–9748.
70 I. Canton, N. J. Warren, A. Chahal, K. Amps, A. Wood, R. Weightman, E. Wang, H. Moore, S. P. Armes, *ACS Cent. Sci.* 2016, **2**, 65–74.
71 L. P. D. Ratcliffe, M. J. Derry, A. Ianiro, R. Tuinier, S. P. Armes, *Angew. Chemie Int. Ed*. 2019, **58**, 2-9
72 R. Laga, O. Janoušková, K. Ulbrich, R. Pola, J. Blažková, S. K. Filippov, T. Etrych, M. Pechar, *Biomacromolecules* 2015, **16**, 2493–2505.
73 M. Save, J. V. M. Weaver, S. P. Armes, P. McKenna, *Macromolecules* 2002, **35**, 1152–1159.

74 K. Skrabania, A. Miasnikova, A. M. Bivigou-Koumba, D. Zehm, A. Laschewsky, *Polym. Chem*. 2011, **2,** 2074–2083.
75 J. Rosselgong, S. P. Armes, W. Barton, D. Price, *Macromolecules* 2009, **42**, 5919–5924.
76 L. P. D. Ratcliffe, A. J. Ryan, S. P. Armes, *Macromolecules* 2013, **46**, 769–777.
77 A. A. Cockram, Novel Block Copolymer Nanoparticles via RAFT Aqueous Emulsion Polymerization, PhD Thesis, University of Sheffield, 2018.
78 H. G. Spencer, *J. Polym. Sci.* 1962, **56**, S25–S28.
79 H. Morawetz, *Macromolecules*, 1996, **29**, 2689–2690.
80 J. R. Lovett, N. J. Warren, L. P. D. Ratcliffe, M. K. Kocik, S. P. Armes*, Angew. Chem. Int. Ed.* 2015, **54**, 1279–1283.
81 N. J. W. Penfold, J. R. Whatley, S. P. Armes, *Macromolecules* 2019, **52**, 1653–1662.
82 O. O. Mykhaylyk, N. J. Warren, A. J. Parnell, G. Pfeifer, J. Laeuger, *J. Polym. Sci. Part B Polym. Phys.* 2016, **54**, 2151–2170.